



EXACT SOLUTION FOR COUPLE STRESS FLUID FLOW PAST A FLUID SPHERE EMBEDDED IN A POROUS MEDIUM WITH SLIP CONDITION

Phani Kumar Meduri¹, Parasa Naga Lakshmi Devi², Vijaya lakshmi Kunche³

¹Department of Mathematics, School of Advanced Sciences, VIT-AP University, Amaravati, Andhra Pradesh, INDIA, phanikumarmeduri@gmail.com

²Department of Mathematics, Institute of Aeronautical Engineering, Dundigal, Hyderabad 500043, Telangana, INDIA, subbusoft2011@gmail.com

³Department of Mathematics, DVR & Dr. HS MIC College of Technology, Kanchikacherla, Vijayawada 521180, Andhra Pradesh, INDIA, vijikunche3@gmail.com

Corresponding Author: ¹Email id: phanikumarmeduri@gmail.com, phani.m@vitap.ac.in

Abstract:

In this paper, using interfacial slip on the boundary, the exact solution is obtained for the Stokes flow through a couple stress fluid sphere which is embedded (implanted) in a porous medium with Brinkman's condition. Analytical computations are derived for the stream functions and drag. For the drag force, special conditions are deduced that satisfy the literature's facts. Graphs are created and the numerical results are tabulated. It is noticed that in the external viscous fluid case the porosity parameter and the drag coefficient are directly correlated and for the external couple stress fluid case with raises in slip parameter the coefficient of drag reduces.

Keywords: viscous fluid, Couple Stress Fluid (CSF), stream function, porous medium, slip condition, drag force.

NOMENCLATURE

p	hydro-static pressure at any point
ρ	density of the fluid
\bar{q}	velocity of the fluid
μ_i, μ_e	fluid viscosities for inner and outer side of the fluid sphere
s	slip parameter
β_1^2	Porosity parameter

Greek symbols

U_∞	velocity at infinity
D_g	drag force
e	couple stress parameter
λ_1^2	Couple stress parameter
μ	viscosity ratio

1. Introduction

The problem of fluid flow through porous surfaces is crucial in oil technology, aquifer recharge, and recharge of ground water. The utilize of beds of porous particles for biological fields like enzyme immobilization or cell and perfusion chromatography to purify proteins, and other biomolecules has attracted a lot of interest as cited by Shukla (2013).

Durlofsky and Brady (1987) in their work developed Green's function to study the behavior of flow in a porous media which helps to determine the effect of flow parameters on hydro dynamically interacting particles in Stokes flow. Padmavathi et al. (1993) used Faxen's law to estimate the torque and drag terms for the flow over a porous sphere. Srinivasacharya and Murthy (2002) used Brinkman's extension equation to investigate the viscous fluid flow past an axisymmetric body implanted within a fluid-impregnated porous region. Partha et al. (2005) have considered the impact of tangential stresses in flows passed through spherical shells and the flow inside the porous region governed by the Brinkman equation. Umavathi et al. (2009) introduced a new method of analysis of strong and weak flows with comparable porosity conditions included with couple stress fluid parameters. Deo et al. (2010) expressed the influence of drag force on a porous structure and stream function was used to numerically analyze the nature of fluid in and outside of the sphere. Kumara (2012) examined the consequence of various types of basic temperature gradients on the criterion for convection initiation in a layer of an non-compressible CSF-saturated porous region. The mathematical formulation demonstrates that the

principle of exchange of firmness probably applies regardless of the shape of the basic temperature profile. Sunil et al. (2013) studied the effect of rotation on a CSF with a generalized energy method. Kumar et al. (2015) discussed about a CSF having appended particles with variable gravity in a porous region. The dispersion relation is analyzed numerically with Rayleigh-Ritz, Cauchy-Schwarz inequality equations and the results are depicted graphically. Eegunjobi and Makinde (2017) work has reported on influence of an assorted convection hydro-magnetic flow of CSF passed through a vertical channel filled with a soaked porous region. Pavlovskaya et al. (2018) in their work used the magnetic resonance imaging (MRI) method to investigate symmetric fluid flow in a porous region in cylinder sections. Prasad and Tina (2021) studied the impact of magnetic fields on Stoke's Newtonian motion over a porous spheroidal particle and the Brinkman model is suggested to rule the flow in porous channels. The applied magnetic field helps in estimating the drag effect on the porous spheroid. Parida et al. (2021) investigated on the steady free convective flow of a nanofluid over a stretching sheet embedded in a porous medium. Murugan and Sekar (2022) considered magnetic field dependent (MFD) approach for a comprehensive understanding of the factors affecting thermos-convective instability in ferromagnetic fluids within a rotating porous medium. Prasad and Priya (2022) have considered the CSF flow over an impervious sphere placed in a porous region with slip condition over the surface and the drag force values were computed analytically. Punnamchandrar and Sitotaw (2022) have developed analytical expressions to estimate the impact of the non-miscible fluid flows in a porous medium with slip at boundaries was graphically.

Murthy and Kumar (2016) have critically analyzed the viscous fluid flow past a surfactant fluid sphere under no-slip conditions. Kishore and Ramdas (2016) in their study used a CFD-based internal solver to examine numerically the heat transfer phenomena of spherical particles in Newtonian fluids with velocity slip and uniform thermal boundary conditions (B. Cs) at the fluid-solid interface. Lakshmi and Kumar (2022) have obtained an analytical solution for drag for a uniform flow past a fluid drop with slip condition. Devi and Kumar (2022, 2023) have obtained an exact solution for CSF flow over a fluid sphere filled with CSF, and partially surfactant CSF sphere with an interfacial slip condition respectively. The drag force illustrates analytically.

The above-mentioned literature work focused on different geometries embedded in porous regions with slip and no-slip conditions. The present work mainly focuses on giving an exact solution for biological applications found in different types of flows like the combination of viscous fluid and CSF sphere implanted in a porous region with slip condition is the new study.

2.1 Fundamental equations:

Consider a fluid sphere containing CSF inner side it, is placed in a flow of uniform viscous fluid far from it. It is presumed that the flow is steady, axisymmetric, and incompressible. The model's geometry is shown in Fig. 1.

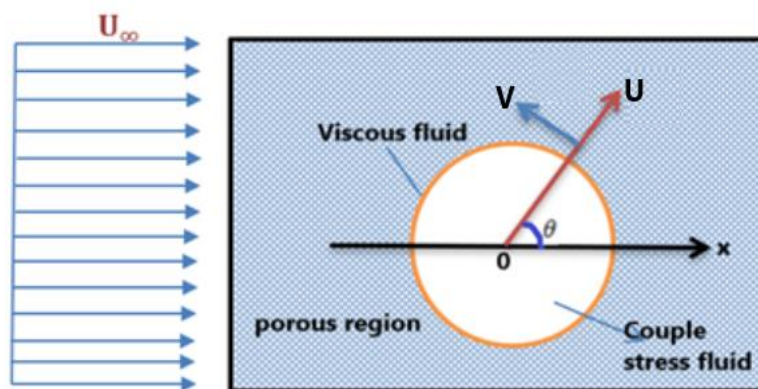


Fig. 1. The geometry of viscous fluid over a CSF sphere implanted in a porous region.

The continuity equation is

$$\nabla \cdot \bar{q} = 0. \tag{1}$$

The field equations that determine the internal flow of couple stress fluid flow are as follows:

$$\nabla^2 \bar{q} = \left(\frac{1}{\mu_i}\right) \nabla P, \tag{2}$$

The momentum equation of external viscous fluid flow in porous region governed by the Brinkman model is

$$\nabla^2 \bar{q} - \left(\frac{\beta_1}{\alpha}\right)^2 \bar{q} = \frac{1}{\mu_e} \nabla P. \tag{3}$$

Due to the geometrical structure of the present problem, we chose a spherical coordinate system as our point of reference. "The scale factors for the system are $h_1 = 1, h_2 = R, h_3 = R \sin\theta$." (Naga Lakshmi Devi and Phani Kumar (2022)).

In axisymmetric flow, U and V are velocity components in terms of stream function are exhibited as

$$U(R, \theta) = \frac{1}{R^2 \sin\theta} \frac{\partial \Psi}{\partial \theta}; V(R, \theta) = \frac{-1}{R \sin\theta} \frac{\partial \Psi}{\partial R}. \tag{4}$$

Eliminating pressure P and using Eq. (4), reduces Eq. (2) and Eq. (3) to,

$$E_0^2 \left[E_0^2 - \frac{\lambda_1^2}{\alpha^2} \right] \Psi = 0, \tag{5}$$

$$E_0^4 \left[E_0^2 - \frac{\beta_1^2}{\alpha^2} \right] \Psi = 0. \tag{6}$$

The non-dimensional scheme is taken in Eq. (5) and Eq. (6) as

$$R = ar; \Psi = \psi U_\infty a^2; P = p \frac{U_\infty \mu}{\alpha}; E_0^2 = \frac{E^2}{\alpha^2}; U = u U_\infty; V = v V_\infty, \text{ porosity parameter } \beta_1^2 = \frac{a^2}{k}.$$

The momentum equation in non-dimensional form is

$$E^2 [E^2 - \lambda_1^2] [E^2 - \beta_1^2] \psi = 0, \tag{7}$$

where, porosity parameter $\beta_1^2 = \frac{a^2}{k}$, couple stress parameter $\lambda_1^2 = \frac{\mu a^2}{\eta}$ and $E^2 \equiv \frac{\partial^2}{\partial r^2} + \frac{1}{r^2} \frac{\partial^2}{\partial \theta^2} - \frac{\cot\theta}{r^2} \frac{\partial}{\partial \theta}$.

As, $\lambda_1^2 \rightarrow \infty$, couple stress fluid tends to viscous fluid, $\beta_1^2 \rightarrow \infty$, porous region reduces to no porous region.

The solution of Eq. (7) which are regular for outer flow (ψ'_{1e}) and for inner flow (ψ'_{1i}) regions by superposition process are given by:

$$\psi'_{1e} = \left[\frac{l_1}{r} + r^2 + m_1 \sqrt{r} K_{\frac{3}{2}}(\beta_1 r) \right] G_2(x), \tag{8}$$

$$\psi'_{1i} = \left[l_2 r^2 + m_2 r^4 + n_2 \sqrt{r} I_{\frac{3}{2}}(\lambda_1 r) \right] G_2(x). \tag{9}$$

Here, $K_{\frac{3}{2}}(x)$ and $I_{\frac{3}{2}}(x)$ represents modified Bessel's functions, $G_2(x)$ is a Gegenbauer functions. (Ramana Murthy, Phani Kumar (2016), Vijaya Lakshmi and Phani Kumar (2022)).

The parameters l_1, m_1, l_2, m_2, n_2 in Eq. (8) and (9) can be found by applying B. Cs:

(i). Regularity conditions:

$$\left. \begin{array}{l} \text{a) } \lim_{r \rightarrow \infty} \psi'_e = \frac{r^2 \sin^2 \theta}{2} \text{ (Outer region)} \\ \text{b) } \lim_{r \rightarrow 0} \psi'_i = \text{Finite (Inner region).} \end{array} \right\} \tag{10}$$

(ii). Impermeability condition: no mass transfer occurs at the fluid sphere's interface on $r = 1$.

$$\psi'_{1e} = \psi'_{1i} = 0. \tag{11}$$

(iii). Slip condition: The tangential stress acting at that location on the surface is related to the tangential velocity of the liquid relative to the solid at that point. (Happel and Brenner (1983)) i.e.,

$$\tau_{r\theta e} = \vartheta (q_\theta - V_{\theta i}), \text{ where } \vartheta \text{ is the sliding friction,} \tag{12}$$

(iv). Shear stress is continuous at crossing the interface of the fluid sphere. i.e.,

$$\tau_{r\theta e} = \tau_{r\theta i}. \tag{13}$$

(v). Type A condition: vanishing of couple stress $m_{r\theta} = 0$ i.e.,

$$\left(\frac{\partial [E^2 \psi']}{\partial r} \right) = \left(e + \frac{1}{r} \right) E^2 \psi'. \tag{14}$$

Here e is the couple stress parameter given by $e = \frac{\eta'}{\eta}$ with ($\eta' \neq \eta$) here η and η' are couple stress viscosity coefficients.

2.2. Calculations:

Using the B. Cs., (10) - (14) in Eq. (8) and Eq. (9), the following five system equations were derived.

$$l_1 = -1 - m'_1;$$

$$l_2 + m_2 + n'_2 = 0;$$

$$\begin{aligned}
 & l_1(4 + s) + m'_1(2 + \beta_1^2 + (2 + s)\Delta_1(\beta_1)) - (n'_2)s(\Delta_2(\lambda_1)) + 2sl_2 + 4sm_2 = 2s + 2; \\
 & 6l_1 + m'_1(4 + \beta_1^2 + 2\Delta_1(\beta_1)) + \mu(-6m_2 - (n'_2)(4 + 2\Delta_2(\lambda_1))) = 0; \\
 & m_2(10 - 10e) - n'_2\lambda_1^2(\Delta_2(\lambda_1) + (1 + e)) = 0;
 \end{aligned} \tag{15}$$

where, $m'_1 = m_1 K_{\frac{3}{2}}(\beta_1)$; $n'_2 = n_2 I_{\frac{3}{2}}(\lambda_1)$, slip parameter $s = \frac{\partial a}{\mu}$, viscosity ratio $\mu = \frac{\mu_i}{\mu_e}$.

Solving Eq. (15) analytically, resulted to

$$m'_1 = \frac{(3s + 6)\phi'_2 - 6\phi'_2}{\Omega}; \quad n'_2 = \frac{6\phi'_1 - (6 + 3s)\phi'_1}{\Omega}; \quad m_2 = n'_2 \Lambda_1, \quad \Lambda_1 = \frac{\lambda_1^2(\Delta_2(\lambda_1) + (1 + e))}{(10 - 10e)}$$

$$\begin{aligned}
 & \text{where, } \Omega = \phi'_1\phi'_2 - \phi'_2\phi'_1, \\
 & \phi'_1 = (-s - 2 + \beta_1^2 + (2 + s)\Delta_1(\beta_1)); \\
 & \phi'_2 = s(-2 + 2\Lambda_1 - \Delta_2(\lambda_1)); \\
 & \phi'_1 = (-2 + \beta_1^2 + 2\Delta_1(\beta_1)); \\
 & \phi'_2 = \mu(-4 + 6\Lambda_1 - 2\Delta_2(\lambda_1));
 \end{aligned}$$

Thus, outer and inner flow stream functions of Eq. (8) and Eq. (9) are derived.

2.3. Evaluation of drag force:

The limiting form of the drag force (D_g) on a body, which is placed in a porous medium can be given by (Satya Deo et al. (2010)).

$$D_g = 4\pi\mu_e U_\infty a \beta_1^2 \lim_{r \rightarrow \infty} \left[\frac{r^3(\psi'_e - \psi^*_\infty)}{\varpi^2} \right], \text{ where, } \varpi^2 = r^2 \sin^2 \theta. \tag{16}$$

In the above Eq. (16), ψ^*_∞ denotes the fluid motion at infinity correlated with the stream function.

Replacing Eq. (8), Eq. (10) in Eq. (16) and apply limiting conditions we get,

$$\begin{aligned}
 D_g &= 2U_\infty\mu_e\pi a\beta_1^2(l_1) \\
 &= 2U_\infty\mu_e\pi a\beta_1^2(-1 - m'_1).
 \end{aligned} \tag{17}$$

Case (i): As slip parameter, $s \rightarrow \infty$, we get D_g without slip condition as

$$D_g = -2U_\infty\mu_e\pi a\beta_1^2 \left(1 + \frac{(18\mu - 12)}{(6\mu)(\Delta_1(\beta_1) - 1) - 2(-2 + \beta_1^2 + 2\Delta_1(\beta_1))} \right) \tag{18}$$

Case (ii): If $\mu \rightarrow \infty$ and using, $\Delta_1(\beta_1) = \frac{1 + \beta_1 + \beta_1^2}{1 + \beta_1}$, Eq. (18) reduces to viscous flow past a solid sphere embedded

in a porous medium without slip condition.

$$D_g = -\pi U_\infty \mu_e \pi a (6\beta_1^2 + 6\beta_1 + 6). \tag{19}$$

Case (iii): If $\beta_1 = 0$ (no porous region). then Eq. (19) reduces to

$$D_g = -(6U_\infty\mu_e\pi a), \tag{20}$$

which is the drag force (D_g) for a flow of viscous fluid over a rigid sphere without slip condition. The above equation also matches with the results of Satya Deo et al. (2010), Happel and Brenner (1983).

Now the coefficient of drag (cd) is calculated as

$$\begin{aligned}
 cd &= \frac{D_g}{\frac{1}{2}\pi\rho U_\infty^2 a^2}, \\
 \therefore cd &= \frac{-6\pi\mu_e U_\infty a}{\frac{1}{2}\pi\rho U_\infty^2 a^2}.
 \end{aligned} \tag{21}$$

When, $s \rightarrow \infty$, $\mu \rightarrow \infty$, and $\beta_1 = 0$, then the coefficient of drag is

$$cd = -\frac{24}{Re}, \text{ with, } Re = \frac{(2a)\rho U_\infty}{\mu_e}. \tag{22}$$

Equation (22) corresponds to the coefficient of drag for a solid sphere without slip condition (Happel and Brenner (1983)).

Additionally, we have acquired drag force of uniform CSF flow beyond a viscous fluid sphere implanted in a porous medium.

3. Exact solution for CSF flow beyond a viscous fluid sphere embedded in a porous medium:

3.1. Problem formulation:

Consider a CSF flow past a viscous fluid sphere placed fixed in a porous region, far from it has a uniform velocity. The flow is presumed to be steady, axisymmetric and non-compressible. The geometry of the model is presented in Fig. 2. as

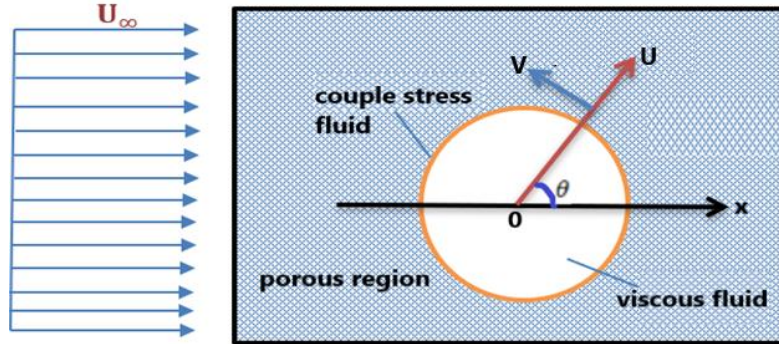


Figure 2: Geometry of CSF over a viscous fluid sphere implanted in a porous region.

For this geometry of the problem, Eqs (1) to Eqs. (7) remain same.

The solution of Eq. (7) which are common for outer flow (ψ''_{2e}) and for inner flow (ψ''_{2i}) regions by superposition procedure are given by:

$$\psi''_{2e} = \left[\frac{l_1}{r} + r^2 + m_1 \sqrt{r} K_{\frac{3}{2}}(\beta_1 r) + n_1 \sqrt{r} K_{\frac{3}{2}}(\lambda_1 r) \right] G_2(x), \quad (23)$$

$$\psi''_{2i} = [l_2 r^2 + m_2 r^4] G_2(x). \quad (24)$$

The parameters l_1, m_1, n_1, l_2, m_2 in Eq. (23), Eq. (24) are obtained by implementing the B. Cs. (10) to (14).

3.2. Calculations:

Using the B.Cs. (10) - (14) in Eq. (23) and Eq. (24) gives the following system of five equations.

$$l_1 + m'_1 + n'_1 = -1,$$

$$l_2 + m_2 = 0,$$

$$\left. \begin{aligned} (6 + s)l_1 + m'_1 \left(\beta_1^2 + 4 + (2 + s)\Delta_1(\beta_1) - \frac{\beta_1^4}{\zeta^2} \right) + n'_1 \left(\lambda_1^2 + 4 + (2 + s)\Delta_1(\lambda_1) - \frac{\lambda_1^4}{\zeta^2} \right) + \\ 2s(l_2 + 2m_2) = 2s, \\ -6l_1 + m'_1 \left(-\beta_1^2 - 4 - 2\Delta_1(\beta_1) + \frac{\beta_1^4}{\zeta^2} \right) + n'_1 \left(-\lambda_1^2 - 4 - 2\Delta_1(\lambda_1) + \frac{\lambda_1^4}{\zeta^2} \right) + 6\mu m_2 = 0, \\ m'_1 \beta_1^2 \{ \Delta_1(\beta_1) + (1 + e) \} + n'_1 \lambda_1^2 \{ \Delta_1(\lambda_1) + (1 + e) \} = 0, \\ \text{where, } m'_1 = m_1 K_{\frac{3}{2}}(\beta_1); \quad n'_1 = n_1 K_{\frac{3}{2}}(\lambda_1). \end{aligned} \right\} \quad (25)$$

Solving Eqs. (25) analytically, results to

$$l_1 = -1 - m'_1 - n'_1, \quad l_2 = -m_2$$

$$m'_1 = \frac{-(3s + 6)\phi'_4 + 6\phi'_4}{\Omega_1}; \quad m_2 = \frac{-6\phi'_3 + (3s + 6)\phi'_3}{\Omega_1}; \quad n'_1 = m'_1 \Lambda_2; \quad \Lambda_2 = \frac{\beta_1^2 (\Delta_1(\beta_1) + (1 + e))}{\lambda_1^2 (\Delta_1(\lambda_1) + (1 + e))};$$

$$\text{where, } \Omega_1 = \phi'_3 \phi'_4 - \phi'_4 \phi'_3,$$

$$\phi'_3 = \left(2 + s - \beta_1^2 - 4 - (2 + s)\Delta_1(\beta_1) + \frac{\beta_1^4}{\zeta^2} \right) + \Lambda_2 \left(\lambda_1^2 - 2 - s + (2 + s)\Delta_1(\lambda_1) - \frac{\lambda_1^4}{\zeta^2} \right);$$

$$\phi'_4 = -2s;$$

$$\phi'_3 = \left(2 - \beta_1^2 - 2\Delta_1(\beta_1) + \frac{\beta_1^4}{\zeta^2} \right) + \Lambda_2 \left(\lambda_1^2 - 2 + 2\Delta_1(\lambda_1) - \frac{\lambda_1^4}{\zeta^2} \right);$$

$$\phi'_4 = 6\mu;$$

Thus, outer and inner flow stream functions of Eq. (23) and (24) are derived.

3.3. Evaluate drag force:

The limiting form of the drag force (D_g) on a body, which is placed in a porous medium can be given by (Satya Deo et al. (2010)).

$$D_g = 4\pi\mu_e U_\infty a \beta_1^2 \lim_{r \rightarrow \infty} \left[\frac{r^3(\psi_e'' - \psi_\infty^*)}{\varpi^2} \right], \text{ where } \varpi^2 = r^2 \sin^2 \theta. \quad (26)$$

In the above Eq. (26), ψ_∞^* as denotes the fluid motion at infinity is correlated with the stream function.

Putting Eq. (23) and Eq. (10) in Eq. (26) and apply limiting conditions we get,

$$D_g = 2U_\infty\mu_e\pi a\beta_1^2(l_1) = 2U_\infty\mu_e\pi a\beta_1^2(-1 - m'_1(\Lambda_2 + 1)). \quad (27)$$

Case (i): As slip parameter, $s \rightarrow \infty$, we get D_g without slip condition as

$$D_g = -2U_\infty\mu_e\pi a\beta_1^2 \left(1 + \frac{(18\mu - 12)}{(6\mu)(\Delta_1(\beta_1) - 1) - 2(-2 + \beta_1^2 + (2\Delta_1(\beta_1)))} \right) \quad (28)$$

Case (ii): If viscosity ratio $\mu \rightarrow \infty$ and using, $\Delta_1(\beta_1) = \frac{1 + \beta_1 + \beta_1^2}{1 + \beta_1}$, Eq. (28) reduces to

$$D_g = -U_\infty\mu_e\pi a(6\beta_1^2 + 6\beta_1 + 6). \quad (29)$$

Case (iii): When porosity parameter, $\beta_1 = 0$, Eq. (29) it is reducing to,

$$D_g = -(6U_\infty\mu_e\pi a), \quad (30)$$

which is the drag force (D_g) for a viscous fluid flow over a solid sphere in a non-porous medium without slip condition. The above equation also matches with the results of Satya Deo et al. (2010), Happel and Brenner (1983).

Now the (cd) coefficient of drag is calculated as

$$cd = \frac{D_g}{\frac{1}{2}\pi\rho U_\infty^2 a^2}, \quad \therefore cd = \frac{-6\pi\mu_e U_\infty a}{\frac{1}{2}\pi\rho U_\infty^2 a^2}. \quad (31)$$

When, $s \rightarrow \infty$, $\mu \rightarrow \infty$, and $\beta_1 = 0$, then cd tends to

$$cd = -\frac{24}{Re}, \text{ with } Re = \frac{(2a)\rho U_\infty}{\mu_e}, \quad (32)$$

Eq. (32) corresponds to the coefficient of drag without slip condition for a solid sphere (Happel and Brenner (1983)). Thus, the obtained results are validated.

4. Results and Discussion:

Case 1: Exact solution for viscous fluid flow beyond a CSF sphere implanted in a porous region:

The stream function values are given in Eqs. (8) and (9) using the B. Cs from (10) – (14) they were derived. In a porous region with slip condition, the drag force (D_g) is calculated as given in Eq. (17), which for special cases are matching with results in existing literature.

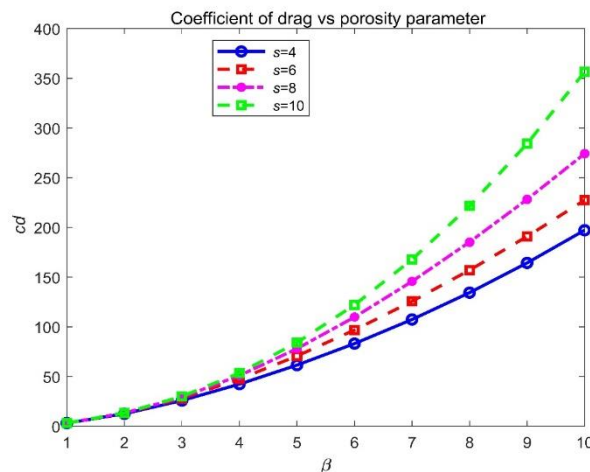


Fig. 3. The coefficient of drag (cd) w.r.t. porous parameter (β) for varying slip parameter (s) at fixed viscosity ratio $\mu = 5$ and couples stress parameter $e = 2$.

The numerical results of coefficient of drag for changing slip and porous parameters at a constant viscosity ratio are displayed and listed in Fig. 3 and Table. 1 respectively. It is observed that the coefficient of drag increases along with the porous parameter values.

Table 1: The coefficient of drag (cd) w.r.t. porous parameter (β) for varying slip parameter (s) at fixed viscosity ratio $\mu = 5$ and couples stress parameter $e = 2$.

$\beta \setminus s \rightarrow$ \downarrow	4	6	8	10
1	3.2348	3.2389	3.2408	3.2419
2	12.5509	13.0602	13.3078	13.4542
3	25.8866	28.0166	29.2376	30.0292
4	42.4040	47.5297	51.0162	53.5414
5	61.5240	70.6748	78.0548	84.1328
6	83.1584	96.8401	109.7945	122.0781
7	107.4083	125.6811	145.7051	167.7447
8	134.4189	157.0545	185.3182	221.6071
9	164.3232	190.9443	228.2466	284.2716
10	197.2277	227.4033	274.1898	356.5112

Case 2: Exact solution for CSF flow beyond a viscous fluid sphere implanted in a porous medium:

The stream functions of CSF flow past a viscous fluid were obtained in Eqs. (23) and (24) using the boundary conditions from (10) - (14). In a porous medium with slip condition and the drag force (D_g) of a CSF past a viscous fluid is calculated as shown in Eq. (27).

The numerical results of coefficient of drag (cd) for changing porous parameter (β) and slip parameters (s) at a constant viscosity ratio (μ) and CSF are displayed and listed in Fig. 4 and Table. 2 respectively. It is noticed that as the slip parameter value rises, the coefficient of drag (cd) values slightly decreases.

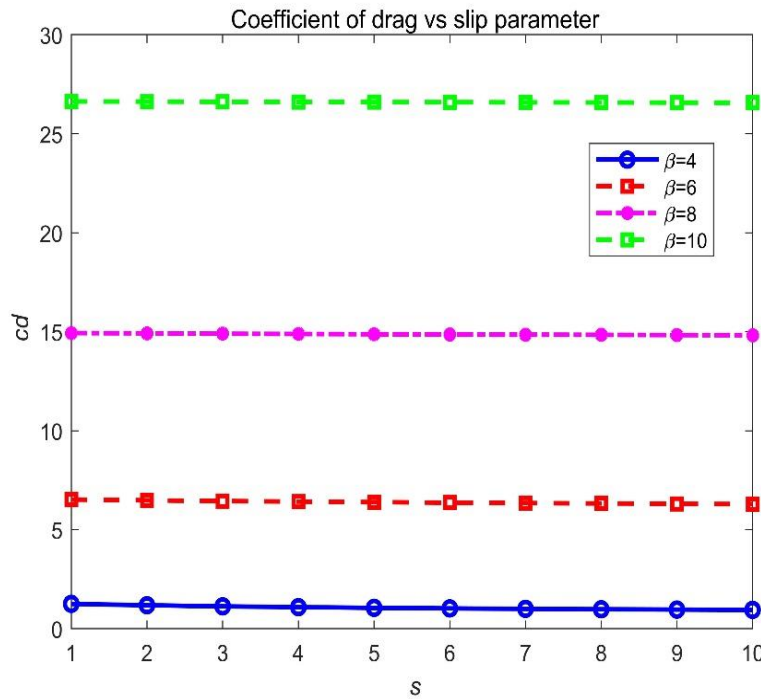


Fig. 4. The (cd) coefficient of drag w.r.t. (s) slip parameter for varying (β) porous parameter at fixed $\mu = 5$ and $e = 2$.

Table 2: The (cd) coefficient of drag w.r.t. (s) slip parameter for varying (β) porous parameter at fixed $\mu = 5$ and $e = 2$.

$s \setminus \beta \rightarrow$ ↓	4	6	8	10
1	1.2558	6.5226	14.9348	26.6299
2	1.1847	6.4835	14.9166	26.6196
3	1.1310	6.4493	14.9004	26.6104
4	1.0888	6.4191	14.8860	26.6022
5	1.0550	6.3922	14.8731	26.5949
6	1.0271	6.3682	14.8614	26.5882
7	1.0039	6.3465	14.8508	26.5822
8	0.9841	6.3269	14.8412	26.5766
9	0.9671	6.3091	14.8323	26.5716
10	0.9524	6.2928	14.8242	26.5669

Case 3: The numerical results of the coefficient of drag (cd) for fixed the porosity parameter $(\beta = 6)$, the slip parameter (s) at constant viscosity ratio (μ) , and the couple stress parameter (e) are displayed and summarized in Fig. 5 and Table 3. The coefficient of drag is observed to progressively increase as the outside of the viscous fluid sphere in slip parameter raises and to significantly decrease when the outside of the CSF sphere in slip parameter raises.

Table 3: A) outside viscous coefficient of drag (cd) and B) outside couple stress coefficient of drag (cd) w.r.t. slip parameter (s) for fixed porosity parameter $(\beta = 6)$, $\mu = 5$ and $e = 2$.

s ↓	A)	B)
1	11.4718	1.2558
3	12.1662	1.131
5	12.5736	1.055
7	12.8415	1.0039
9	13.0311	0.9671
11	13.1723	0.9395
13	13.2815	0.9179
15	13.3685	0.9005
17	13.4395	0.8863
19	13.4985	0.8745
21	13.5483	0.8644
23	13.5909	0.8558
25	13.6278	0.8483
27	13.66	0.8418
29	13.6884	0.836
31	13.7136	0.8308
33	13.7361	0.8262
35	13.7564	0.8221
37	13.7747	0.8183
39	13.7913	0.8149

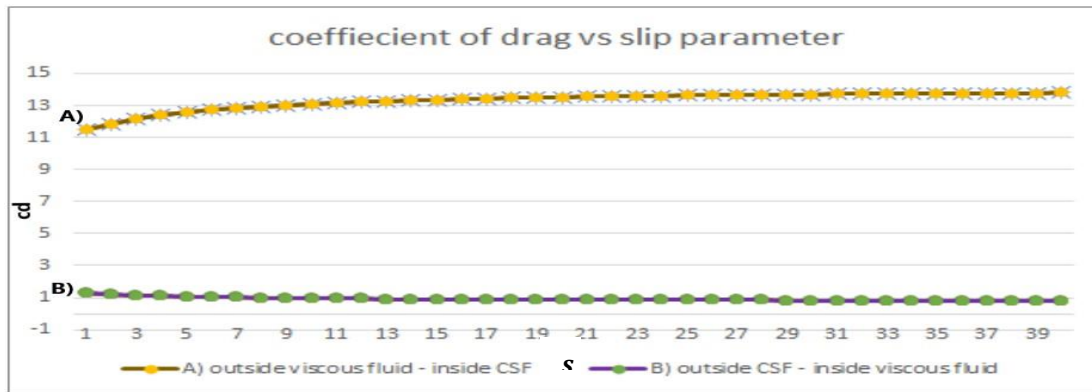


Fig. 5: A) viscous coefficient of drag (cd) and B) couple stress (cd) coefficient of drag w.r.t. (s) slip parameter for fixed porosity parameter ($\beta = 6$), $\mu = 5$ and $e = 2$.

5. Conclusions:

The summary of the work are as follows:

- i. We have been able to infer an analytical solution in this work for the uniform flow of a viscous fluid beyond a CSF sphere in a porous region where the surface has a slip condition, and vice versa. For these situations, the inner and outer stream functions and drag force were analytically calculated. Results of special conditions i.e., no slip condition when $s \rightarrow \infty$, a solid sphere case when $\mu \rightarrow \infty$, and no porous zone for $\beta = 0$ are deduced and observed consistent with data in literature.
- ii. In the case of an outer viscous fluid, it is observed that changing the slip parameter (s) and the porous parameter (β_1) led to a rise in the co-efficient of drag values for those variables, respectively. There is a drop in coefficient of drag values for modifying various parameters in the outer CSF case varying porosity parameter (β_1) slip parameter (s).
- iii. It has been shown that viscous fluid flow beyond a CSF sphere in a porous zone with slip parameter exhibits higher coefficient of drag (cd) values compared to its opposite flow.

The obtained exact solutions for creeping flow are useful to the researchers to compare their results for moderate Reynolds numbers using numerical methods like Finite Difference Method (FDM), Finite Element Method (FEM) etc., which have applications in chemical engineering, biological studies etc. Other non-Newtonian fluids can be used to extend the work.

References

- Bitla, P. and Sitotaw, F. Y. (2022): Effects of Slip and Inclined Magnetic Field on the Flow of Immiscible Fluids (Couple Stress Fluid and Jeffrey Fluid) in a Porous Channel, *Journal of Applied Mathematics*, Vol. 2022, Article ID. 2799773, pp. 1-11. <https://dx.doi.org/10.1155/2022/2799773>
- Brenner, H. (1983): *Low Reynolds number hydrodynamics*, Nijhoff publications. <https://dx.doi.org/10.1007/978-94-009-8352-6>
- Choudhary, S.S. and Mahajan, A. (2013): Conditional stability for thermal convection in a rotating couple-stress fluid saturating a porous medium with temperature and pressure dependent viscosity, *Journal of Geophysics and Engineering*, Vol. 10, pp. 1-11. <http://dx.doi.org/10.1088/1742-2132/10/4/045013>
- Deo, S., Shukla, P. and Gupta, B. R. (2010): Drag on a Fluid Sphere Embedded in a Porous Medium, *Advances in Theoretical Applied Mechanics*, Vol. 3, No. 1, pp. 45 – 52.
- Devi, P. N. L. and Meduri, P. K. (2022): Drag Over a fluid sphere filled with couple stress due to flow of a couple stress fluid with slip condition, *Trends in Sciences*, Vol. 19, No. 24, pp. 1-12. <https://dx.doi.org/10.48048/tis.2022.3133>
- Devi, P. N. L. D. and Meduri, P. K. (2023): Couple stress fluid past a contaminated fluid sphere with slip condition, *Applied Mathematics and Computation*, Vol. 446, pp. 1-12. <https://dx.doi.org/10.1016/j.amc.2023.127845>

- Durlofsky, L. and Brady, J. F. (1987): Analysis of the Brinkman equation as a model for flow in porous media, *American Institute of Physics*, Vol. 30, No. 11, pp. 3329-3341. <https://dx.doi.org/10.1063/1.866465>
- Eegunjobi, A.S and Makinde, O.D. (2017): Irreversibility analysis of hydromagnetic flow of couple stress fluid with radiative heat in a channel filled with a porous medium, *Results in Physics*, Vol. 7, pp. 459-469. <https://dx.doi.org/10.1016/j.rinp.2017.01.002> ,<https://dx.doi.org/10.1002/zamm.202100340>
- Kishore, N. and Ramteke, R. R. (2016): Forced convective heat transfer from spheres to Newtonian fluids in steady axisymmetric flow regime with velocity slip at fluid solid interface, *International journal thermal science*, Vol. 105, pp. 206–217. <http://dx.doi.org/10.1016/j.ijthermalsci.2016.03.009>
- Kumar, K., Singh, V. and Sharma, S. (2015): On the Onset of Convection in a Dusty Couple-Stress Fluid with Variable Gravity through a Porous Medium in Hydro magnetics, *Journal of Applied Fluid Mechanics*, Vol. 8, No. 1, pp. 55-63. <https://dx.doi.org/10.36884/jafm.8.01.21642>
- Kumara, I.S.S., Sureshkumar, S. and Devaraju, N. (2012): Effect of Non-Uniform Temperature Gradients on the Onset of Convection in a Couple-Stress Fluid-Saturated Porous Medium, *Journal of Applied Fluid Mechanics*, Vol. 5, No. 1, pp. 49-55.
- Lakshmi K, V. and Meduri, P. K. (2022): Stokes flow of Micropolar fluid beyond fluid sphere with slip condition, *Zeitschrift fur angewandte Mathematik und Physik*, Vol. 102, pp.1-11.
- Madasu, K. P. and Sarkar, P. (2022): Couple stress fluid past a sphere embedded in a porous medium, *Archive of Mechanical Engineering*, Vol. 69, No. 1, pp. 5–19. <https://dx.doi.org/10.24425/ame.2021.139314>
- Murthy, J.V.R. and Meduri, P. K. (2016): Exact solution for flow over a contaminated fluid sphere for stokes flow, *Journal of Physics-Conference series*, Vol. 662, 012016. <https://dx.doi.org/10.1088/1742-6596/662/1/012016>
- Murugan, D. and Sekar, R. (2022): An Analytical Study of Linear Stability Analysis on Soret Driven Ferro thermohaline Convection in A Darcy Porous Medium with MFD Viscosity and Coriolis Force, *Journal of Naval Architecture and Marine Engineering*, Vol. 19, pp. 83-96. <http://dx.doi.org/10.3329/jname.v19i2.40593>
- Padmavathi, B.S., Amarnath, T., and Nigam, S. D. (1993): Stokes Flow past a Porous Sphere using Brinkman's model, *Zeitschrift fur angewandte Mathematik und Physik*, Vol. 44, pp. 929–939. https://ui.adsabs.harvard.edu/link_gateway/1993ZaMP...44..929P <https://dx.doi.org/10.1007/BF00942818>
- Parida, B. C, Swain, B. K, Senapati, N. (2021): Mass Transfer Effect on Viscous Dissipative Mhd Flow of Nanofluid Over a Stretching Sheet Embedded In A Porous Medium, *Journal of Naval Architecture and Marine Engineering*, Vol. 18, pp. 73-82. <https://dx.doi.org/10.3329/jname.v18i1.53380>
- Partha, M., Murthy, K. P. V. S. N., and Sekhar, G. P. R. (2005): Viscous Flow past a Porous Spherical Shell-Effect of Stress Jump Boundary Condition, *Journal of Engineering Mechanics*, Vol. 131, pp. 1291-1301. [https://dx.doi.org/10.1061/\(ASCE\)0733-9399\(2005\)131:12\(1291\)](https://dx.doi.org/10.1061/(ASCE)0733-9399(2005)131:12(1291))
- Pavlovskaya, G. E., Meersmann, T., Jin, J. and Rigby, S. P. (2018): Fluid flow in a porous medium with transverse permeability discontinuity, *Physical Review Fluids*, Vol. 3, No. 4, pp. 1-20. <https://dx.doi.org/10.1103/PhysRevFluids.3.044102>
- Prasad, M. K. and Bucha, T. (2021): Effect of magnetic field on the slow motion of a porous spheroid: Brinkman's model, *Archive Applied Mechanics*, Vol. 91, pp. 1739–1755. <https://dx.doi.org/10.1007/s00419-020-01852-7>
- Shukla. P. (2013): Creeping flow past a porous sphere with solid pore embedded in porous medium, *Applied Mathematics*, Vol. 59, pp. 15427-15431.
- Srinivasacharya, D. and Murthy J.V.R. (2002): Flow past an axisymmetric body embedded in a saturated porous medium, *C. R. Mecanique*, Vol. 330, pp. 417–423.
- Umavathi, J.C., Kumar, J.P. and Chamkha, J.A. (2009): Convective flow of two immiscible viscous and couple stress permeable fluids through a vertical channel, *Turkish Journal of Engineering an Environmental Sciences*, Vol. 33, pp. 221-43. <https://dx.doi.org/10.3906/muh-0905-29>